

# **Electrochemical oxidation of isothiazolinone biocides and their interaction with cysteine**

Mercedes Ruiz Montoya<sup>1</sup>, Inmaculada Giráldez<sup>2</sup>, Emilio Morales<sup>2</sup>, Rafael Estévez Brito<sup>3</sup> and José Miguel Rodríguez Mellado<sup>3,\*</sup>

<sup>1</sup>Departamento de Ingeniería Química, Química Física y Ciencias de los Materiales, Escuela Técnica Superior de Ingeniería, Centro de Investigación en Tecnología de Productos y Procesos Químicos (Pro2TecS), Campus El Carmen, Universidad de Huelva, E-21071, Huelva, Spain.

<sup>2</sup>Departamento de Química “Prof. J.C. Vilchez Martín”, Facultad de Ciencias Experimentales, Centro de Investigación en Tecnología de Productos y Procesos Químicos (Pro2TecS), Campus El Carmen, Universidad de Huelva, E-21071, Huelva, Spain.

<sup>3</sup>Departamento de Química Física y Termodinámica Aplicada. Instituto Universitario de Investigación en Química Fina y Nanoquímica IUIQFN, CeIA3, Campus Universitario Rabanales, edificio Marie Curie. Universidad de Córdoba. E-14014-Córdoba, Spain.

\*Corresponding author (e-mail: [jmrodriguez@uco.es](mailto:jmrodriguez@uco.es), ORCID: 0000-0002-7639-5040)

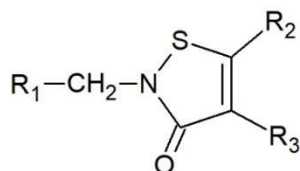
## **Abstract**

This paper presents voltammetric studies on carbon electrodes (linear-sweep cyclic voltammetry and differential pulse voltammetry) on the electrooxidation of methylisothiazolinone (MIT), Chloromethylisothiazolinone (CMIT) and 4,5-dichloro-2-octyl-4-isothiazolin-3-one (DCOIT). The oxidation products have been identified after electrolysis of the compounds using liquid-liquid extraction and gas chromatography coupled to mass spectrophotometry. The identified compounds for the three biocides correspond in all cases to two-electron processes, with opening of the ring. Adsorption processes were observed for CMIT. From the differential pulse voltammetric results a general reaction pathway is proposed in which the rate-determining step is a chemical reaction placed after the first partially irreversible electron transfer. The interaction of cysteine with MIT and CMIT was studied by differential pulse voltammetry in order to quantify them and the 1:3 mixture. The specificity of the interaction with cysteine and the low values of the peak potentials minimize the interferences. The quantification is made from the decrease of the oxidation signal of cysteine as the biocide concentration increases, being the method adequate for the study of usual cosmetic and household products.

**Keywords:** Isothiazolinone biocides; MIT; CMIT; DCOIT; KATHON; electrolysis; Liquid-liquid extraction coupled with Gas chromatography

## 1. Introduction

A biocide is a substance (from chemical and/or biological origin) able to destroy, inhibit, make harmless, or control harmful organisms. Derivatives of isothiazolinone as methylisothiazolinone (MIT), chloromethylisothiazolinone (CMIT) and 4,5-dichloro-2-octyl-4-isothiazolin-3-one (DCOIT) are widely used as biocidal active ingredients to prevent growth of bacteria in cosmetics (eye shadows, moisturizers and make-up removers) and toiletry [1-4], hair and skin care products, water-desalination reverse osmosis plants [5], adhesives [6,7], biodiesels [8], cooling water treatment [9-11], hydraulic fracturing fluids [12, 13], laundry detergents [14], water-based paints [15], paper for food packaging [16], etc.



MIT:  $R_1=H$ ,  $R_2=H$ ,  $R_3=H$       CMIT:  $R_1=H$ ,  $R_2=Cl$ ,  $R_3=H$       DCOIT:  $R_1=Heptyl-$ ,  $R_2=Cl$ ,  $R_3=Cl$

The wide use of biocides can originate health problems because these chemicals are known contact allergens that cause skin irritation [5, 6, 17, 18] and both oral and inhalation toxicity [13].

The mechanism of action of isothiazolinones is two-step, consisting in a rapid inhibition occurring in minutes of growth and metabolism, followed by a slow irreversible cell damage, which can occur in several hours [19]. The reactivity of MIT and CMIT against glutathione [20] and thiols in general [21, 22] has been reported. At physiological pH the biocides interacted oxidatively with thiols to form disulphides, the following step being the opening of the ring [21]. Chlorinated derivatives do not react with thiols, but their reaction with thiolates is fast [22], this implying that the pH of the medium is essential for the reaction. 5-chloroisothiazolones and isothiazolones inhibit thiol containing enzymes and makes them excellent candidates for activity-based protein profiling of these enzymes [22-24].

HPLC/MS analysis has been used to establish the levels of MIT, CMIT, DCOIT and other biocides [25, 26]. A simple method for measuring DCOIT in marine sediments to very low concentration level has been developed. It consists of a focused ultrasound assisted extraction (FUSE) followed by a solid phase extraction (SPE) clean-up and a stir bar sorptive extraction (SBSE) preconcentration step using thermal desorption system (TD) coupled to GC-MS/MS and provides good recovery [27].

Han et al. used an PbO<sub>2</sub> anode supported on a titanium plate to oxidize wastewater polluted with isothiazolinone biocides [28]. The voltammetric behaviour of isothiazolin-3-ones at boron-doped diamond electrodes (BDD) was reported [29]. In this study it was concluded that the hydroxyl radicals generated at BDD surface were responsible for the degradation of the biocides, being the rate of degradation virtually independent of pH. No other electrochemical studies on these biocides can be found in the literature.

The aim of this work was, first, to establish the mechanisms of the electrochemical oxidation of the isothiazolinone biocides MIT, CMIT and DCOIT on carbon electrodes and, second, to explore the use the interaction with cysteine to quantify these biocides. To achieve these goals, voltammetric measurements, in cyclic and differential pulse modes, together bulk electrolyses are made in buffered solutions, and Liquid-liquid extraction coupled with Gas chromatography is used for the product identification.

## **2. Experimental**

### *2.1. Reagents*

All chemicals used were of Merck analytical grade reagents, with the exception of (*R*)-2-amino-3-mercaptopropionic (L-cysteine), acid 2-methyl-4-isothiazolin-3-one (MIT) and 4,5-

dichloro-2-octyl-isothiazolone (DCOIT) that were from Sigma-Aldrich and 5-chloro-2-methyl-4-isothiazolin-3-one (CMIT) that was from Cymit, and were used without further purification.

## 2.2. Electrochemical measurements

As supporting electrolytes, solutions containing 0.1 M in phosphoric acid were used except in the experiences in which cysteine was present. In this case, phosphate buffer solutions containing 0.05 M in both  $\text{KH}_2\text{PO}_4$  and  $\text{K}_2\text{HPO}_4$  were used. Due to the low solubility of DCOIT in water, the stock solution was prepared in ethanol, with 30% ethanol needed in the cell to avoid its precipitation.

The aqueous solutions were prepared using ultrapure water type I (resistivity 18.2  $\text{M}\Omega\cdot\text{cm}$  at 298 K) obtained from an ultrapure water Millipore system. Ionic strength was adjusted to 0.3 M with  $\text{KNO}_3$ . Stock solutions of MIT, CMIT, DCOIT and cysteine were stored in the dark at 277 K to avoid decomposition. For DCOIT stock solution was prepared in ethanol due to its low water solubility. pH measurements were made prior each experiment with a Crison Basic 20 pH-meter, calibrated daily with the corresponding pH standards (Crison). The pH adjustment was made with solid NaOH.

The electrochemical measurements were made on a CHI650A electrochemical workstation from IJCambria. A three-electrode cell equipped with a Pt wire counter electrode BAS MF-2079, a BAS MF-2079  $\text{Ag}|\text{AgCl}|\text{KCl}$  (3M) reference electrode and a glassy carbon electrode (GCE) from IJCambria ( $7.5\text{mm}^2$  area) working electrode was used. The surface of the electrode was treated with diamond ( $0.25\ \mu\text{m}$ ) and alumina ( $0.3$  and  $0.05\ \mu\text{m}$ ) slurries. Residual material was removed from the electrode surface by sonication in a pure water bath for 30 min after each polishing. Solutions were purged with purified  $\text{N}_2$  for at least 15 min to avoid the presence of oxygen that could originate undesired redox reactions on the electrode. The working concentration was 1 mM for MIT and DCOIT and 3mM for CMIT, with the evident exception of experiments in which the effect of the concentration was studied. All tests were performed at 298 K.

The parameters for differential pulse voltammetry (DPV) were: pulse amplitude 0.05 V, pulse width 0.05 s and pulse period 0.1 s.

The controlled-potential electrolysis was made on a working electrode consisting of a high-density graphite rod of 99.995% purity (Aldrich, CAS number 7782-42-5 C) protected with a silicone tube, which allow to use a cylinder with an area of 75.4 mm<sup>2</sup>. The electrode was polished with a silicon carbide paper, followed by alumina (0.3µm) slurry. Residual polishing material was removed from the surface by sonication of the electrode in an ultrapure water bath for 20 minutes after each polishing. The counter electrode was a stainless-steel rod and the reference electrode a BAS MF-2079 Ag|AgCl|KCl (3M).

The electrolyses were made under continuous stirring with volumes of 10 mL of 1mM biocides (for DCOIT 4% ethanol in cell was necessary for dissolution) and recording the cyclic voltammograms along the electrolysis to check the evolution of biocide. High density graphite rods (GRE) of 99.995% purity form of 6 mm diameter protected with a silicone tube Aldrich (CAS number 7782-42-5 C) were used. The electrode was polished with a silicon carbide paper, followed by alumina (0.3 µm) slurry. Residual polishing material was removed from the surface by sonication of the electrode in a water bath for 10 minutes. Electrolyses were performed until at least 80% of the initial biocide was lost.

### *2.3. Liquid-liquid extraction and Gas chromatography*

An aliquot (300 µL) of the electrolysis solution was placed in a 2 mL vial and extracted by shaking vigorously with 200 µL chloroform for 5 min. The organic phase was dried with anhydrous sodium sulphate. The organic layer was transferred into a new vial.

Aliquots (1 µL) of extracts were injected into a Shimadzu GC-MS (GCMS-TQ8030) equipped with an Agilent HP-5MS fused silica capillary column (30m x 0.25mm i.d., 0.25 mm film thickness). The gas chromatograph system was equipped with a split/splitless injection port operating in splitless mode. The oven temperature program was as follows: The column was kept

at 50 °C for 3 min, ramped at 20 °C min<sup>-1</sup> to 200 °C, held for 5 min and then increased at 40 °C min<sup>-1</sup> to 280 °C and held for 10 min. Helium at a constant flow rate of 1 mL min<sup>-1</sup> was used as the carrier gas. The temperatures of the injector, transfer line and ion source were maintained at 250, 280 and 230 °C, respectively. A solvent delay of 3 min was selected. The carrier gas was helium with a constant flow of 1 mLmin<sup>-1</sup> (mean velocity 36, cms<sup>-1</sup>). The mass spectrometer was performed with electron ionization (EI) at 70 eV, operating in scan mode (50-300 amu). Identification of compounds after electrolysis and DCOIT standard was achieved using the mass spectra. MIT and CMIT standard mass spectra were compared with the data system library (NIST 11).

### 3. Results and discussion

In linear-sweep cyclic voltammetry (LSCV) on a glassy carbon electrode, MIT exhibits one oxidation peak at potentials very close to the discharge of the supporting electrolyte. The influence of the concentration of MIT was studied at two pH values in order to evaluate what is the appropriate working concentration. As it is shows in Figure 1, the peak is deformed at potentials beyond the peak potential due to the overlapping with the discharge of the supporting electrolyte. In differential pulse voltammetry (DPV), the peak appears well defined at the highest concentrations used. For this reason, differential pulse voltammetry is selected as study technique, and 1·10<sup>-3</sup> M as working concentration for MIT.

-- Figure 1 --

DP voltammograms of CMIT at pH 7.00 show an oxidation peak preceded by a shoulder at potentials lower than the peak potential (Figure 2). The DPV obtained at different concentrations lead us to choose a working concentration of 3·10<sup>-3</sup> M. At this concentration the peak appears defined enough to allow its analysis.

-- Figure 2 --

DCOIT is not soluble in water but it is soluble in ethanol. A 30% ethanol in the medium allows us to use concentrations of  $1 \cdot 10^{-3}$  M. In these conditions, the DPV peaks are very close to the discharge of the supporting electrolyte. Attempts have been made to increase the concentration by increasing the percentage of ethanol in cell, but the voltammograms are poorly defined. Therefore, the chosen working concentration was  $1 \cdot 10^{-3}$  M.

The oxidation of MIT was studied in the range of pH 2-11, although at  $\text{pH} > 8.5$  the differential pulse voltammograms are difficult to measure, due to the appearance of wide peaks of and low intensities at potentials immediately lower than the oxidation peak potential, which make difficult the measurement of the peak parameters (Figures S1 and S2 in the Supplementary material).

As previously said, differential pulse voltammetry was revealed as the most reliable technique for the study of the oxidation process, because the well definition and low distortion of the signal. The equation 1, corresponding to first-order processes, was used for the analysis of the DP voltammograms [30]:

$$I = 4I_P[L/(1 + L)^2] \quad (1)$$

where  $L = \exp[-(E-E_P)/b]$ ,  $I_P$  and  $E_P$  being the peak intensity and the peak potential, respectively, and  $b$  is a parameter which has the same value and meaning as the slope of the dc logarithmic analysis [30, 31].

This equation corresponds to a symmetrical peak, which area is proportional to both the number of electrons involved in the process and the reactant concentration.

The variations of peak area and peak potential with pH below pH 8.5 are shown in Figure 3. The areas shown in this figure have been normalized with respect to concentration, because different concentrations are used for MIT and CMIT; so, the comparison between both behaviors can be made more straightly. As can be seen, for MIT the peak area remains roughly constant

throughout the pH range studied. The peak potential remains practically constant up to pH 6 and above this pH value decreases slightly with a slope of  $-18.7$  mV per pH unit.

-- Figure 3 --

For CMIT, the oxidation was studied also in the range of pH 2-11, the differential pulse voltammograms showing two overlapped peaks (Figures S3 and S4 in the Supplementary material). The analysis of the differential pulse voltammograms with equation 1 leads to the appearance of two peaks (named peak 1 and peak 2 attending the potentials at which they appear). The evolution of peak potentials and peak areas with pH corresponding to these peaks can be seen in Figure 3. Again, and for both peaks, the peak area remains practically independent of pH, while the peak potentials remain constant at pH  $<6$ , decreasing very slowly at higher pH values with slopes of  $-13.7$  mV per pH unit, for peak 1, and  $-7.9$  mV per pH unit for peak 2. Moreover, peak 2 has a normalized area similar to that of MIT, whereas the normalized area of peak 1 is c.a. one half than the area of peak 2.

Figure 4A shows the comparison of the voltammograms corresponding to MIT, CMIT and a mixture of both at pH 7.10. As can be seen, the oxidation peak of MIT appears at the same potentials as the peak 1 of CMIT. When comparing the CMIT voltammogram with that of the mixture of both compounds, an intensity increase is observed at potentials corresponding to peak 1 of CMIT. From this behavior it could be concluded that both peaks correspond to the same type of electrochemical process for both compounds, though other explanations can be given, as will be made in the following discussion.

-- Figure 4 --

DCOIT cannot be studied in neutral and basic media. Under these conditions, the  $-\text{COOH}$  group is dissociated and a colloid is formed, which is observed experimentally, with the  $-\text{COO}^-$  groups disposed towards the interior. The voltammograms appear deformed at potentials

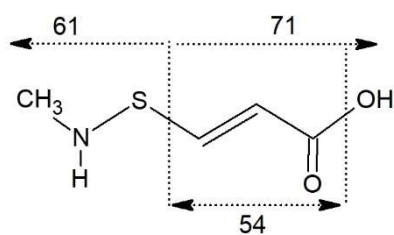
immediately above the peak potential and its analysis is not possible at  $\text{pH} > 6.0$ . At  $\text{pH} \leq 6.0$ , a single peak appears whose peak potential and peak area practically do not vary with  $\text{pH}$ . Figure 4B shows the comparison of the peaks obtained for MIT, CMIT and DCOIT at  $\text{pH} 6.0$ .

Figure 5 shows the curve-fitting of equation 1 to the experimental DP voltammograms for MIT, CMIT and a mixture of both compounds. The fitting between theoretical and experimental data is good in the first part of the curve, but the end part is distorted by the discharge of the supporting electrolyte. The  $b$  values were obtained from the fitting of the experimental results to equation 1 in the first part of the DPV peak. Such  $b$  values were of 75-80 mV for the only MIT peak also for peak 1 and peak 2 of CMIT, somewhat higher than that corresponding to a two-electron process of ECE type, where the r.d.s. is a chemical step after the first reversible electron transfer (60 mV), but much lower than that corresponding to an irreversible one-electron transfer (120 mV) [29, 30]. This behaviour can be attributed to the quasi-reversibility of the transfer, which increases the  $b$  values. In the case of the mixture, the same peaks appear as for CMIT, but peak 1 has a higher intensity due to the presence of MIT. For DCOIT the  $b$  value was 60 mV at  $2.00 < \text{pH} < 6.00$ , this indicating that the process is of ECE type and the reversibility of the transfer is higher than for the other biocides.

-- Figure 5 --

To identify the oxidation products, electrolyses were made at 1.65 V (that is, at potentials higher than those of the oxidation peaks) and in the conditions given in the experimental section. The results of the analyses are given in Figure 6 to 8. Figures S5 to S8 in supplementary material show the gas chromatograms corresponding to the biocides and the oxidation products.

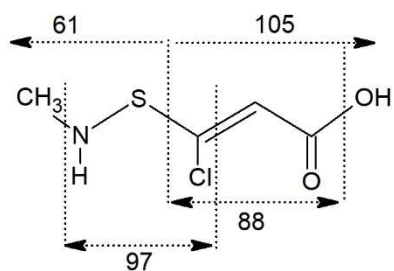
MIT mass spectrum showed molecular ion at  $m/z=115$  [M] and a fragmentation pattern corresponding to MIT (Figure 6A). In the case of MIT electrolysis product (Figure 6B), the identified compound was the following:



This compound has a molecular weight ( $m/z=133$ ), and the spectrum showed the peaks at  $m/z=71$  [ $M-CNSH_4$ ] ion,  $m/z=61$ , [ $CNSH_4$ ] ion and  $m/z=54$ , [ $\cdot C_3H_2O$ ] (Figure 6b).

-- Figure 6 --

CMIT mass spectrum (Figure 7A) showed a molecular ion peak at  $m/z=149$  [ $M$ ] and a fragmentation pattern corresponding to CMIT. For CMIT electrolysis compound the identified compound was the following:



This molecule has a molecular weight of  $m/z=167$ . The fragmentation pattern is shown in Figure 7B. Peaks were observed at  $m/z=105$ , [ $M-C_3ClH_2OH$ ] ion,  $m/z=61$ , [ $CNSH_4$ ] ion,  $m/z=97$  [ $CCINSH_4$ ] ion, and  $m/z=54$  [ $\cdot C_3ClHO$ ].

-- Figure 7 --

DCOIT mass spectrum showed three ions (between 60 and 100 % of relative abundance), at  $m/z$  169 [ $M-C_8H_{16}$ ] ion,  $m/z$  246 [ $M-Cl$ ] ion and  $m/z$  182 [ $MC_7H_{15}$ ] ion. The  $m/z$  281 molecular ion had a low abundance (15 %) (Figure 8A). The identified electrolysis compound for DCOIT was:





Different –SH containing compounds have been tested and finally cysteine (Cys) was selected attending to the potentials measured, solubility and cost. The pH of measurement was near to 7, but the behaviour at other pH values is similar to that will be described below.

Figure 10 shows the effect of the addition of increasing concentrations of biocides to Cys solutions. The oxidation signal of Cys decreases as the biocide concentration increases. This signal is suppressed at biocide concentrations c.a. one half of the Cys concentration used. This agrees with the interaction mechanism proposed by Collier et al. [21] in which two Cys molecules react with one biocide to give the end product.

-- Figure 10 --

As it is shown in Figure 10, this effect occurs irrespective the Cys concentration used. So, the decrease could be used to quantify the biocides as it is presented in Figure 11 and Figure S8 of the supplementary material.

-- Figure 11 --

By varying the Cys concentration, different ranges of biocide concentration can be achieved. As it has been pointed out in the introduction, the main use of these biocides is in 1:3 mixtures of MIT and CMIT,

This MIX is used in different doses for different uses. So, in cosmetic and household products, the doses can reach until 15 ppm [4, 32]. For example, shampoos contain 1.5-14.1 ppm of MIX, baby liquid soap 4.7-6.8 ppm, detergents around 6 ppm and wood surface cleaners c.a. 11 ppm [4]. All these contents are in the range of application of the electrochemical measurements shown in Figure 11. It is true that for other applications as the treatment of biofilms the doses are lower, below 1.2 ppm [33], this meaning that the parameters of the electrochemical method must be optimized for these cases.

#### **4. Conclusions**

The voltammetric study on carbon electrodes of the oxidation of biocides MIT, CMIT and DCOIT allowed to propose a reaction scheme for these processes. From the electrolysis of the biocides, oxidation products have been determined by liquid-liquid extraction and gas chromatography coupled to mass spectrometry. In all cases the oxidation leads to the opening of the ring and the identified compounds correspond to bielectronic processes. At the scheme, the rate-determining step is a chemical reaction placed after the first electron transfer. This transfer is not completely reversible and contributes in part to the kinetics. The study in differential pulse voltammetry of the interaction of cysteine with MIT, CMIT and the mixture of both, allows the quantification of these compounds. The low oxidation values at which the peaks appear and the specificity of the interaction with cysteine minimize the interferences. The cosmetic and household products have mixture contents in the range of validity of the proposed method, but the parameters of the electrochemical method could be optimized to quantify lower values.

#### **5. Acknowledgements**

Financial supports from FEDER, Junta de Andalucía (Research Groups FQM-0198 and RNM371), Ministerio de Economía y Competitividad (research project CTQ-2015-68813R) and Instituto Universitario de Investigación en Química Fina y Nanoquímica IUIQFN, are gratefully acknowledged.

## 6. References

- [1] D. R. Karsa, Biocides, Handbook for Cleaning/Decontamination of Surfaces I. Johansson and P. Somasundaran (Editors), 2007 Elsevier B.V.
- [2] J. J. Zeelle, T. J. McCarthy, Antioxidants multifunctional preservatives for cosmetic and toiletry formulations, *Cosmetics and Toiletries* 98 (1983) 51-55.
- [3] A. B. Law, J. N. Moss, E. E. Lashen, Kathon CG: A new single component broad spectrum preservative system for cosmetics and toiletries, *Cosmetics Science Technology Series I.* (1984) 129-141.
- [4] G. Alvarez-Rivera, T. Dagnac, M. Lores, C. Garcia-Jares, L. Sanchez-Prado L, J.P. Lamas JP, M. Llompart, Determination of isothiazolinone preservatives in cosmetics and household products by matrix solid-phase dispersion followed by high-performance liquid chromatography-tandem mass spectrometry. *J. Chromatogr. A.* 1270 (2012) 41-50. doi:10.1016/j.chroma.2012.10.063.
- [5] M. Isaksson, B. Gruvberger, M. Bruze, Patch testing with serial dilutions of various isothiazolinones in patients hypersensitive to methylchloroisothiazolinone/methylisothiazolinone. *Contact Dermat.* 70 (2014) 270-275. doi: 10.1111/cod.12184
- [6] M. Isaksson, B. Gruvberger, M. Bruze, Occupational contact allergy and dermatitis from methylisothiazolinone after contact with wallcovering glue and after a chemical burn from a biocide. *Dermatitis* 15(4) (2004) 201-205. doi: 10.2310/6620.2004.04017
- [7] M. C. Goodier, L.-Y. Zang, P. D. Siegel, E. M. Warshaw, Isothiazolinone Content of US Consumer Adhesives: Ultrahigh-Performance Liquid Chromatographic Mass Spectrometry Analysis, *Dermatitis* 30 (2019) 129-134. doi: 10.1097/DER.0000000000000455

- [8] G. V. S. Luz, B. A. S. M. Sousa, A. V. Guedes, C. C. Barreto, L. M. Brasil, Biocides Used as Additives to Biodiesels and Their Risks to the Environment and Public Health: A Review, *Molecules* 23 (2018) 2698. doi:10.3390/molecules23102698
- [9] K. M. Wiencek, T. M. Williams, R. F. Semet, A New Biocide for Control of Algal Biofouling in Cooling Towers, *Cooling Tower Institute Journal*, 19(2) (1998), 56
- [10] C. L. Wiatr, Detection and eradication of a nonLegionella pathogen in a cooling water system, *The Analyst*, IX (2002) 38-48.
- [11] M. Critchley, R. Bentham, The efficacy of biocides and other chemical additives in cooling water systems in the control of amoebae, *J. Appl. Microbiol.* 106 (2009) 784–789
- [12] Y. Lester, T. Yacob, I. Morrissey, K. G. Linden, Can we treat hydraulic fracturing flowback with a conventional biological process? The case of guar gum. *Environ. Sci. Technol. Lett.* 1(1) (2013) 133–136 doi: 10.1021/ez4000115.
- [13] G. A. Kahrilas, J. Blotevogel, P. S. Stewart, T. Borch, Biocides in hydraulic fracturing fluids: A critical review of their usage, mobility, degradation, and toxicity. *Environ. Sci. Technol.* 49 (2015) 16-32. doi: dx.doi.org/10.1021/es503724k
- [14] House Hold Products Database (2015) <https://www.householdproducts.nlm.nih.gov/cgi-bin/household/brands?tbl=brands&id=19039040> (accessed July 4, 2019)
- [15] M. D. Lundov, B. Kolarik, R. Bossi, L. Gunnarsen, J. D. Johansen, Emission of isothiazolinones from water-based paints, *Environ. Sci. Technol.* 48 (2014) 6989–6994. doi: dx.doi.org/10.1021/es500236m
- [16] Q. B. Lin, T. J. Wang, H. Song, B. Li, Analysis of isothiazolinone biocides in paper for food packaging by ultra-high-performance liquid chromatography-tandem mass spectrometry, *Food*

Addit. Contam. Part. A Chem. Anal. Control. Expo. Risk Assess, 27(12) (2010) 1775-81. doi: 10.1080/19440049.2010.521896.

[17] D.A. Basketter, R. Rodford, I. Kimber, I. Smith, J.E. Wahlberg, Skin sensitization risk assessment: A comparative evaluation of 3 isothiazolinone biocides. Contact Dermatitis 40 (1999) 150-154. doi: 10.1111/j.1600-0536.1999.tb06013.x

[18] A. Boyapati, M. Tam, B. Tate, A. Lee, A. Palmer, R. Nixon, Allergic contact dermatitis to methylisothiazolinone: exposure from baby wipes causing hand dermatitis. Australas. J. Dermatol. 54 (2913) 264-267. doi: 10.1111/ajd.12062.

[19] T. M. Williams, The Mechanism of Action of Isothiazolone Biocides, Power Plant Chemistry 9 (2007) 14-22

[20] P.J. Collier, A.J. Ramsey, P. Austin, P. Gilbert, Growth inhibitory and biocidal activity of some isothiazolone biocides. Journal of Applied Bacteriology 69 (1990) 569-577

[21] P.J. Collier, A. Ramsey, R.D. Waigh, K.T. Douglas, P. Austin, P. Gilbert, Chemical reactivity of some isothiazolone biocides, Journal of Applied Bacteriology 69 (1990) 578-584

[22] M. Ghizzoni, H. J. Haisma, F. J. Dekker, Reactivity of isothiazolones and isothiazolone-1-oxides in the inhibition of the PCAF histone acetyltransferase, European Journal of Medicinal Chemistry 44 (2009) 4855–4861. doi:10.1016/j.ejmech.2009.07.025

[23] P.J. Collier, P. Austin, P. Gilbert, Isothiazolone biocides: enzyme-inhibiting pro-drugs, International Journal of Pharmaceutics, 73 (1991) 195-201

[24] R. Wisastra, M. Ghizzoni,<sup>a</sup> H. Maarsingh, A. J. Minnaard, H. J. Haismaa, F. J. Dekker, Isothiazolones; thiol-reactive inhibitors of cysteine protease cathepsin B and histone acetyltransferase PCAF, Organic & Biomolecular Chemistry 9 (2011) 1817-1822. doi: 10.1039/c0ob00464b

- [25] Q: B. Lin, T.J. Wang, H. Song, B. Li, Analysis of isothiazolinone biocides in paper for food packaging by ultra-high-performance liquid chromatography-tandem mass spectrometry, *Food Addit. Contam. Part A Chem. Anal. Control Expo. Risk Assess*, 27(12) (2010), 1775-1781. doi: 10.1080/19440049.2010.521896.
- [26] J. J. Heo, U.-J. Kim, J.-E. Oh, Simultaneous quantitative analysis of four isothiazolinones and 3-iodo-2-propynyl butyl carbamate in hygienic consumer products, *Environ. Eng. Res.* 24(1) (2019) 137-143 doi: doi.org/10.4491/eer.2018.14
- [27] E. García, I. Giráldez, M. Ruiz Montoya, E. Morales, Determination of five booster biocides in sediments by focused ultrasound-assisted extraction and stir bar sorptive extraction–thermal desorption–gas chromatography–mass spectrometry. *Microchem. J.* 152 (2020) 104445 doi: doi.org/10.1016/j.microc.2019.104445
- [28] W. Q. Han, L. J. Wang, X. Y. Sun, J. S. Li, Treatment of bactericide wastewater by combined process chemical coagulation, electrochemical oxidation and membrane bioreactor, *Journal of Hazardous Materials* 151 (2008) 306-315. doi:10.1016/j.jhazmat.2007.05.088
- [29] V. Kandavelu. S. Yoshihara, M. Kumaravel, M. Muruganathan, Anodic oxidation of isothiazolin-3-ones in aqueous medium by using boron-doped diamond electrode. *Diamond & Related Materials* 69 (2016) 152-159. doi:10.1016/j.diamond.2016.08.008
- [30] J. M. Rodríguez Mellado, M. Blázquez, M. Domínguez, J. J. Ruiz, Derivation and experimental verification of approximate explicit equations in differential pulse polarography. I. First order processes, *J. Electroanal. Chem.*, 195 (1985) 263-270. doi:10.1016/0022-0728(85)80047-4
- [31] J. M. Rodríguez Mellado, M. Blázquez, M. Domínguez, Derivation and experimental verification of approximate explicit equations in differential pulse polarography. III. Diagnostic criteria for characterization of first-order processes, *J. Electroanal. Chem.*, 241 (1988) 291-295. doi: doi.org/10.1016/0022-0728(88)85132-5

[32] Regulation (EC) No. 1223/2009 of the European Parliament and of the Council of 30 November 2009 on cosmetic products (recast), Off. J. Eur. Union L342 (2009) 59

[33] B. Corbin, Biofouling control in industrial water systems, CTI Journal, 38(2) (2017) 8-14

## Figure headings

**Figure 1.** Voltammograms of MIT at different concentrations. (A) Cyclic voltammograms at pH 5.0,  $v=0.1 \text{ V}\cdot\text{s}^{-1}$ . (B) Cyclic voltammograms at pH 7.47,  $v=0.1 \text{ V}\cdot\text{s}^{-1}$ . (C) DP voltammograms at pH 5.0. (D) DP voltammograms at pH 7.47.

**Figure 2.** DP voltammograms of CMIT at different concentrations. pH=7.00.

**Figure 3.** DP voltammetry. Variation of peak area with pH. The areas have been normalized with respect to concentration. ( $\circ$ ) MIT; ( $\bullet$ ) CMIT, peak 1; ( $\blacksquare$ ) CMIT, peak 2

**Figure 4.** A) Comparison of the DP voltammograms of MIT, CMIT and a 1:3 mixture of both biocides. pH7.10. (B) Comparison of the DP voltammograms of MIT, CMIT and DCOIT. pH=6.00.

**Figure 5.** Curve-fitting of equation 1 to experimental DP voltammograms for: (from top to bottom)  $9.1 \times 10^{-4} \text{ M}$  MIT;  $2.73 \times 10^{-3} \text{ M}$  CMIT; a mixture of  $2.73 \times 10^{-3} \text{ M}$  CMIT and  $9.1 \times 10^{-4} \text{ M}$  MIT.

**Figure 6.** Mass spectra. (A) MIT; (B) MIT electrolysis product.

**Figure 7.** Mass spectra. (A) CMIT; (B) CMIT electrolysis product.

**Figure 8.** Mass spectra. (A) DCOIT; (B) DCOIT electrolysis product.

**Figure 9.** Variation of the peak area with the CMIT concentration. pH = 7.00.

**Figure 10.** Interaction of biocides with cysteine in  $0.5 \text{ M KH}_2\text{PO}_4 + 0.5 \text{ M K}_2\text{HPO}_4$  buffer. Black continuous line: DP voltammograms of cysteine. (A) DP voltammograms of 1 mM cysteine with different concentrations of MIT. (B) DP voltammograms of 5 mM cysteine with different concentrations of CMIT. (C) DP voltammograms of 1 mM cysteine with mixtures of both MIT and CMIT in the ratio 1:3. Biocide concentrations are indicated in the figures.

**Figure 11.** Differences between the currents measured at 0.54 V and that obtained for cysteine in the absence of biocide. Biocide concentrations corresponding to Figure 10C.